Reema Gupta, Monika Tomar, Vinay Gupta*, Yuan Zhou, Anuj Chopra, Shashank Priya, A. S. Bhalla and R. Guo

Giant Magnetoelectric Effect in PZT Thin Film Deposited on Nickel

DOI 10.1515/ehs-2015-0010

Abstract: The magnetoelectric (ME) effect has been investigated in lead zirconate titanate (PZT) thin film deposited on nickel foil using chemical solution deposition (CSD) technique. The synthesized PZT thin films are found to possess perovskite structure without presence of any intermediate layer. PZT thin film deposited on nickel foil exhibits a good ferroelectric property with a high remnant polarization of about 86 $\mu C/cm^2$.The ferroelectric loop has been modeled using domain wall theory to verify the behavior of the ferroelectric domains. It is observed that deposition conditions, specially annealing temperature, play a crucial role in enhancing the magnetoelectric effect. A high ME coefficient of 220 $mVcm^{-1}Oe^{-1}$ at a bias magnetic field of 50 Oe has been obtained due to enhanced magnetoelectric coupling between PZT film and nickel foil.

Keywords: ferroelectric, lead zirconium titanate, magnetoelectric effect, and nickel foil

Introduction

Recent surge in the use of wireless electronics and sensor nodes has led to rapid demand in development of alternative power sources. Reliability on batteries in many of these applications is a limiting factor in the deployment of the wireless devices due to their short lifetime. Solar cells and micro-windmills have been developed to utilize the freely available environmental energy for powering electronics (Priya and Inmam 2009). Several other sources of energy are being globally investigated including vibrations, magnetic fields, thermal energy, water flow, and human body (Gilbert and Galouchi 2008; Stanner and Paradiso 2004). Among these choices, one of the attractive direction of research is utilizing electromagnetic radiations for energy harvesting using magnetoelectric effect (ME) (Ryu et al. 2002; Martins and Mendez 2013). Magnetoelectric effect implies induction of the electric polarization $(\vec{P})$ upon applying magnetic field $(\vec{H})$ or vice-versa. ME effect in composite materials that consist of both piezoelectric and magnetostrictive phases has attracted extensive research interests in recent years (Eerenstein, Mathur, and Scott 2006), due to their possible use in various other applications besides energy harvesting (Chen et al. 2010; Jeon et al. 2003).

Recently, it has been demonstrated that using Nickel (Ni)/$Pb(Zr,Ti)O_3$ (PZT) based ME laminate cantilever structure, one can efficiently harvest both vibration and magnetic field simultaneously (Zhou, Apo, and Priya 2013; Patil et al. 2014). Thus, these composites are promising for producing electricity from the weak magnetic field present in the surrounding. Moreover, the simple laminate structure provides great potential toward device miniaturization. Among the various choices for perovskite ferroelectrics, PZT is known to possess excellent electromechanical properties (Gubinyi et al. 2008). PZT thin films have been extensively studied using both physical (Bouregba et al. 2000), and chemical vapor deposition (CVD) techniques (Foster et al. 1997) for various applications such as MEMS devices, sensors (Bouregba et al. 2000), and non-volatile random access memories (Foster et al. 1997). PZT thin film has been deposited on various metalized substrates like platinized silicon (Meng et al. 2000), stainless steel (Oikawa et al. 1976), and titanium (Zou, Ruda, and Yacobi 2001) etc. resulting in wide variation in morphology as well as the dielectric and piezoelectric properties. With the focus on future power sources for wireless sensor nodes, the possibility of PZT integration on nickel foils is the goal of this study. Nickel is known to have large magnetostriction coefficient (McCorkle 1923) and offers low lattice mismatch with the PZT such that one can accommodate the interfacial strain within the deposited structure.

***Corresponding author: Vinay Gupta,** Department of Physics and Astrophysics, University of Delhi, Delhi 110007, India, E-mail: drguptavinay@gmail.com

Reema Gupta, Department of Physics and Astrophysics, University of Delhi, Delhi 110007, India

Monika Tomar, Physics Department, Miranda House, University of Delhi, Delhi 110007, India

Yuan Zhou, Anuj Chopra, Shashank Priya, Bio-inspired Materials and Devices Laboratory (BMDL), Center for Energy Harvesting Materials and Systems (CEHMS), Virginia Tech, Blacksburg, VA 24061, USA

A. S. Bhalla, R. Guo, Materials Research Laboratory, The Pennsylvania State University, University Park, PA 16802, USA

Limited studies have been conducted on magnetoelectric effects of chemical solution deposited PZT films on nickel substrate (Chashin et al. 2008; Bi, He, and Wang 2012; Li et al. 2012). Li et al (2012) have studied the ME response of the bilayer (PZT/Ni) developed on silicon substrate using Kerr effect, but the reported response was very weak as compared to other reports (Bi, He, and Wang 2012). A magnetoelectric coefficient of 50 mV/cm.Oe for PZT/Ni structure synthesized on titanium buffered Si was reported by Bi, He, and Wang (2012). He, Wang, and Bi (2010) have obtained high value of ME coefficient (3 V/cm.Oe) but with an additional titanium as buffer layer. This demonstrates that a high magnetoelectric response can be observed either by using an additional buffer layer or by optimizing the growth conditions for PZT on magnetic substrates.

Experimental

Lead zirconium titanate thin films were deposited on nickel substrate using chemical solution deposition technique (Dutschke and Meinhardt 2004). A 0.4 M of $Pb_{1.1}(Zr_{0.6}Ti_{0.4})O_3$ (PZT) sol was prepared from lead (Pb), zirconium (Zr) and titanium (Ti) precursors in a glove box. The details of solution preparation process are discussed elsewhere (Park et al. 2005). Before deposition, the nickel foil was polished and cleaned with isopropyl alcohol (IPA) and acetone. The prepared PZT solution was spin-coated repeatedly on a polished Ni substrate ($1.5 \times 1.5 \times 0.02\,cm^3$). PZT thin film with thickness of 1 μm was obtained through successive pyrolysis (300 °C) and annealing steps. The film was annealed using a vertical rapid thermal annealing process at different temperatures (600 °C, 650 °C and 700 °C). For electrical measurements, 100 nm thick platinum (Pt) circular electrodes of 200 μm diameter were deposited on the sample surface through a shadow mask by RF sputtering at room temperature. The metal-ferroelectric-metal (MFM) capacitor configuration (Pt-PZT-Ni) was formed with PZT film poled transversely by the corona poling process (Marshall, Zhang, and Whatmore 2008).

X-ray diffraction (XRD) (Bruker) with Cu Kα radiation (λ = 1.5406 Å) was used for crystallographic studies. Field emission scanning electron microscope (FESEM) was used to study the surface morphology of deposited films. The polarization-electric field (P-E) hysteresis loops were measured for all the synthesized films. Atomic force microscopy (Dimension Icon AFM, Bruker) and piezoelectric force microscopy (PFM) measurements were performed to study the surface morphology and piezoelectric properties. The dielectric and ferroelectric properties were obtained using impedance analyzer (HP4194A, USA) and Sawyer-Tower bridge (Radiant) arrangement, respectively. The ME voltage coefficient was measured using a homebuilt system that comprises of a lock-in-amplifier, an electromagnet, Helmholtz coil and a Gauss meter. The sample was placed in the center of the Helmholtz coil (H_{ac}) which itself was located in the center of an electromagnet (H_{dc}). The ME effect was measured in L-T mode (longitudinally magnetized and transversely poled) configuration with a time varying DC magnetic field in the presence of AC magnetic field (1 Oe, 1 kHz).

Results and Discussions

Figure 1 shows the XRD pattern and FESEM images of PZT films annealed at three different temperatures (600 °C, 650 °C, and 700 °C) on nickel substrate. A poor crystallinity and the presence of pyrochlore phase (Py) was observed for the PZT films annealed at low temperature (<650 °C) as shown in Figure 1(a). Similar to XRD investigations, film deposited at low temperatures was also found to exhibit poor crystallinity in SEM analysis, as shown in Figure 1(d). PZT film annealed at 650 °C shows XRD peaks (Figure 1(b)) corresponding to the (100), (110) and (111) crystalline planes of the rhombohedral structure (Abdelghafar et al. 2000) at $2\theta \approx 21.8^o$, 30.6^o and 38.1^o, respectively. The PZT film annealed at 650 °C shows a pure perovskite phase without any parasitic/pyrochlore phase. Furthermore, PZT thin film annealed at 650 °C shows a preferred growth (73 %) along (110) plane. The SEM image (Figure 1(e)) shows good granular structure confirming crystallinity at optimized annealing temperature of 650 °C. The film annealed at 700 °C exhibited the presence of nickel oxide in addition to pure perovskite PZT phase indicating inter-diffusion of oxide layer with Ni as shown in Figure 1(c). It has been reported in literature that the inter-diffusion of nickel oxide in dielectric film results in deterioration of magnetoelectric response. The microstructure of PZT thin film annealed at 700 °C was observed to be entirely different (Figure 1(f)) in comparison to the microstructure observed for PZT film annealed at 650 °C. PZT film annealed at 700 °C was found to have distribution of clusters resulting in the formation of leafy fractal morphology as shown in the SEM image. The calculated value of lattice constant "*a*" using Lebail method was 4.09 Å for the PZT thin film

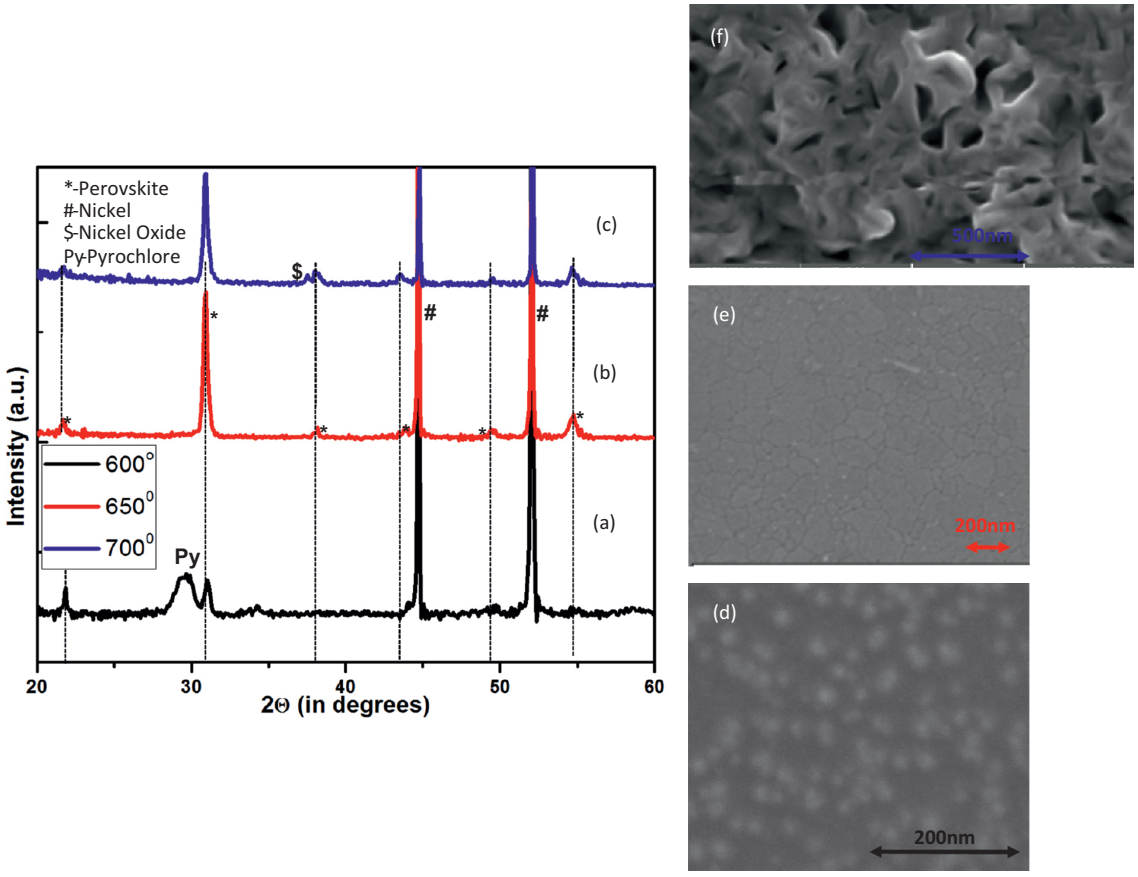

Figure 1: (a), (b) and (c) shows the XRD patterns of the PZT thin film annealed at 600 °C, 650 °C and 700 ° and (d), (e) and (f) shows the corresponding FESEM images of surface of PZT thin film.

annealed at optimized temperature (650 °C). The obtained value of lattice parameters are close to the corresponding values ($a = 4.05$ Å) reported for bulk PZT (Vrejoiu et al. 2007). The average crystallite size determined from XRD pattern by using full width at half maximum value of the dominant XRD peak (110) was found to be about 26 nm (Patterson 1939).

Figure 2 illustrates the ferroelectric polarization-electric field (P-E) hysteresis loop for the deposited PZT thin films in metal-ferroelectric-metal (MFM) configuration. It has been observed that all the PZT films show P-E hysteresis loops irrespective of their annealing temperature as shown in Figure 2(a). PZT film annealed at 650 °C exhibits well saturated square shaped P-E hysteresis loop (Park et al. 2004) with enhanced values of remnant polarization (P_r), saturation polarization (P_s) and coercive field (E_c) of about 86 μC/cm^2, 100 μC/cm^2 and 110 kV/cm, respectively. The remnant polarization values observed for the films are 2 times higher as compared to the values reported in the literature for the PZT films annealed under similar conditions (Polcawich and McKinstry 2000; Bi, Zhang, and Fan 2007). Therefore, highly pronounced ferroelectric hysteresis loops have been obtained for PZT thin films annealed at optimum temperature of 650 °C in the present study. The PZT thin films annealed at 600 °C and 700 °C were observed to be leaky in nature and possessed lower polarization as shown in Figure 2(a). This is possibly due to the parasitic phases present at both 600 °C and 700 °C as observed in XRD measurements. The P-E loops were found to be slightly asymmetrical along both the polarization and applied field axis due to the asymmetrical top and bottom electrode configuration (Misirlioglu, Okatan, and Alpay 2010). The study indicates that annealing temperature plays a crucial role in tailoring the properties of PZT thin film Ni substrate (Es-Souni and Piorra et al. 2001).

The experimentally obtained P-E hysteresis loop of thin film deposited on Ni substrate (annealed at 600 °C) was fitted with expression derived using the domain wall switching theory (Massad and Smith 2003) as shown in Figure 2(b). The theory predicts the hysteresis behavior based on the energy losses at domain wall pinning sites

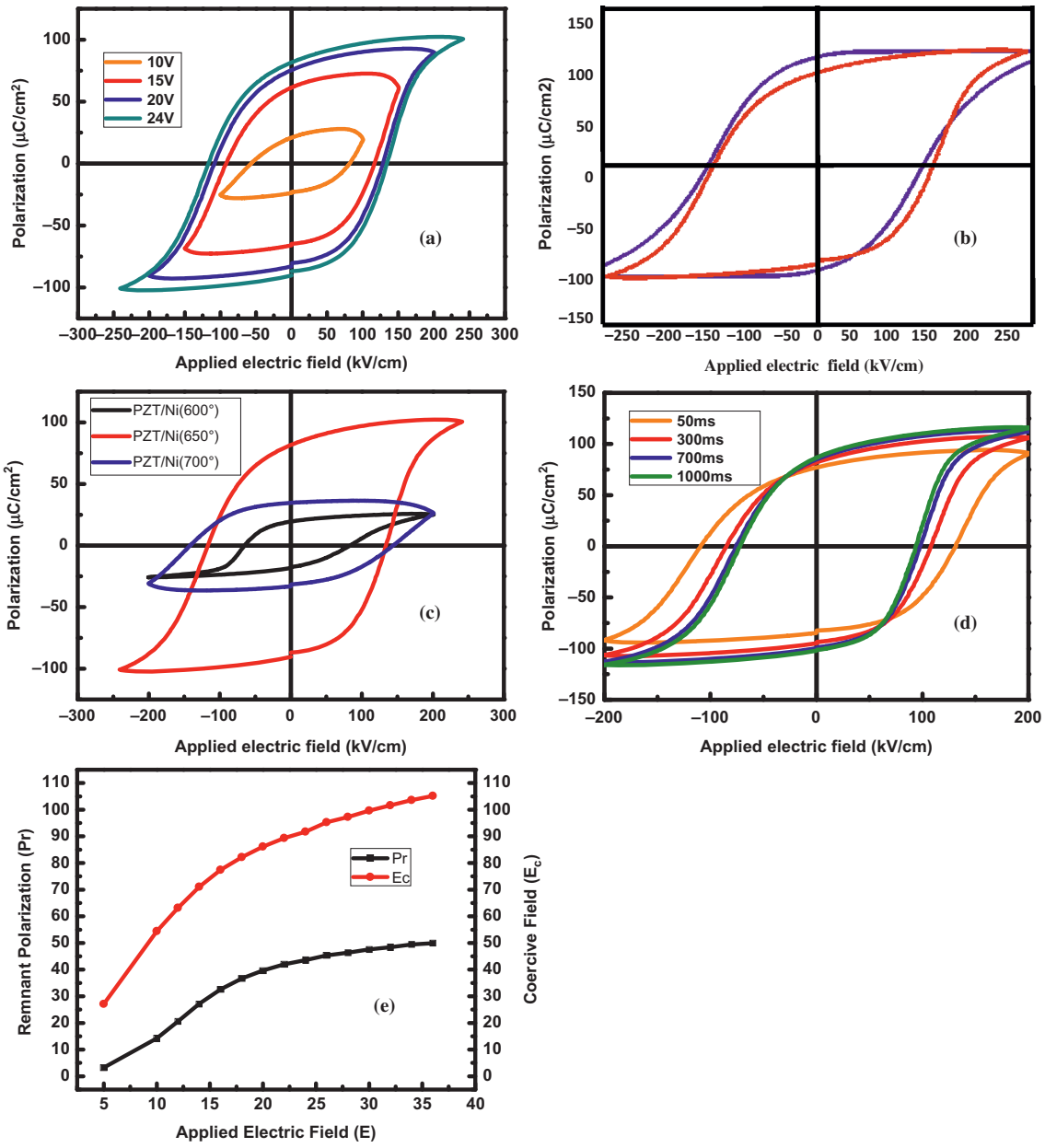

Figure 2: (a) PE hysteresis loops for the PZT/Ni samples annealed at three different temperatures, (b) Measured and theoretically fitted PE loop for the PZT film annealed at 650 °C, (c) and (d) show the effect of frequency and amplitude of applied electric field on the PE loop of the optimized PZT film, (e) shows the variation of remnant polarization (P_r) and coercive field (E_c) with applied electric field.

(Massad and Smith 2003). The model was developed under the premise that the applied electric field produces a force which acts on the walls of the domains and deforms it analogous to a pinned membrane. The anhysteretic polarization P_{an} obtained using the Langevin Model can be expressed as (Massad and Smith 2003):

$$P_{an} = P_s\left[Coth\left(\frac{E}{a}\right) - \left(\frac{a}{E}\right)\right] \quad [1]$$

Where P_s is the saturating polarization as obtained from the experimental data, E is the applied electric field and "a" is the shape parameter for P_{an} incorporating the relative thermal effects which are balanced with the electrostatic energy to model the anhysteretic polarization. The hysteretic equation for irreversible changes in polarization can be given as:

$$\frac{dP_{irr}}{dt} = \frac{dE}{dt}\cdot\frac{\tilde{\delta}[P_{an} - P_{irr}]}{k\delta - \alpha[P_{an} - P_{irr}]} \quad [2]$$

where δ is the direction parameter having the value $+1$ for $\frac{dP}{dt} > 0$ and -1 for $\frac{dP}{dt} < 0$. This ensures that the energy

required to overcome the pinning sites always opposes changes in polarization and $\tilde{\delta}$ is defined as:

$$\tilde{\delta} = \begin{cases} 1; & \{dE > 0 \text{ and } P > P_{an}\} \text{ or } \{dE < 0 \text{ and } P < P_{an}\} \\ 0; & \text{otherwise} \end{cases}$$

"k" is the average energy required to overcome the pinning sites, and "α" is the parameter quantifying domain interaction. Reversible polarization (P_{rev}) is defined in terms of reversibility coefficient (c), anhysteretic polarization (P_{an}) and irreversible polarization (P_{irr}) as:

$$P_{rev} = c[P_{an} - P_{irr}] \quad [3]$$

The net polarization (P) being the resultant of reversible and irreversible polarization is expressed as:

$$P = P_{rev} + P_{irr} \quad [4]$$

The first component of polarization i. e. reversible polarization (P_{rev}) models the effects of domain wall bending. The measured P-E hysteresis loop has been fitted to the domain wall theory using eqs [1]–[4]. The solution to the differential eq. [2] has been solved using Runga Kutta 4th order polynomial method in MATLAB. The P-E loop obtained from the theoretical model was found to fit well with the measured loop for PZT thin film annealed at 650 °C (Figure 2(b)). Various hysteresis loop parameters including shape parameter, domain interaction and average energy required for pinning were calculated from the best fitting of hysteresis loop. The value of "α" was found to be about 1.1 × 10^6 Vcm/C which represents the domain coupling present in the thin film (Massad and Smith 2003). The estimated value of "k" and "a" are 150 μC/cm^2 and 170 μC/cm^2 respectively. The obtained value of saturation polarization and the average energy required for pinning the domain sites from the theoretical fitting is similar to that obtained from the experimental data. This performance is superior to that reported in the literature (Pandey et al. 2005), and confirms that higher polarization can be obtained by maximizing the domain interactions within the films. Figure 2(c) shows the frequency dependent hysteresis loops obtained for the PZT thin film annealed at 650 °C. It can be seen from Figure 2 (c) that with decrease in frequency resulted in higher saturation polarization. Also, the coercive field was found to decrease from 109 kV/cm to 72 kV/cm with decrease in frequency from 20 Hz to 1 Hz (Figure 2(c)). Figure 2(d) shows the P-E hysteresis curves obtained for PZT thin film annealed at 650 °C with different magnitude of applied electric fields from 20 to 240 kV/cm. It can be found from (Figure 2(d)) that the loops at 20 Hz are well saturated at high electric fields indicating a good ferroelectric behavior which can be attributed to the better crystallinity and dense microstructure. With increase in the magnitude of applied electric field, remnant polarization as well as coercive field were found to increase as shown in the Figure 2(e) having a maximum value of 50 μC/cm^2 and 105 kV/cm, respectively at an applied voltage of 24 V. A sharp enhancement is observed in both P_r and E_c upto 15 V and saturation is observed for the higher applied voltages. The observed behavior of E_c and P_r is similar to those reported for various ferroelectric thin films and ceramics (Ambika et al. 2012; Qiu et al. 2002), indicating that the deposited PZT thin film on Ni substrate has high break down field (>240 kV/cm).The value of remnant polarization (86 μC/cm^2) obtained for the deposited PZT thin films is higher than the corresponding values obtained for sol-gel deposited PZT thin film on nickel alloy (36.8 μC/cm^2) (Seifert et al. 2004) or PLD deposited epitaxial film (19.6 μC/cm^2) (Kambale et al. 2013).

The measured frequency dependent dielectric constant (ϵ') and corresponding losses (ϵ'') of the PZT thin film are shown in Figure 3(a). It can be observed from Figure 3(a) that the PZT thin film has a high dielectric

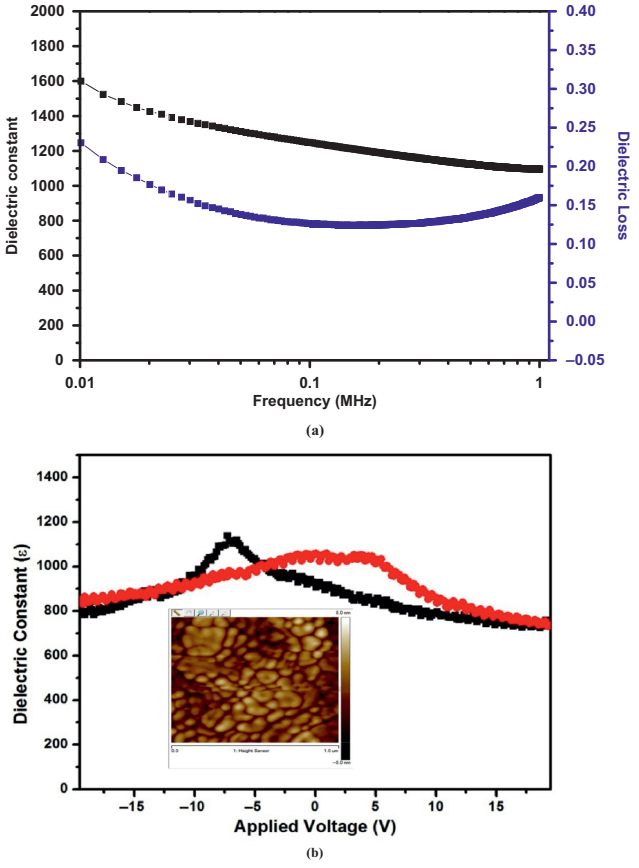

Figure 3: (a) Variation of dielectric and dielectric loss with frequency in log scale for the PZT film (b) Dielectric constant-applied voltage hysteresis loop. Inset shows the AFM micro-image of the PZT thin film deposited on Ni Substrate.

constant (1,150) and low loss (0.15) over a wide range of frequency (>100 kHz), showing a low frequency dispersion as required for potential device applications. The results indicate the absence of any barrier layer at the metal-dielectric interface and depict the good quality of deposited PZT thin films with minimum defects. The low lattice mismatch (0.15) of PZT with underneath Ni substrate may be responsible for the better nucleation of PZT and hence, preferred (110) oriented growth (Figure 1) that leads to high dielectric constant. The obtained value of dielectric constant (~1,150) is higher as compared to the corresponding reported values (1,000) for (110) oriented PZT thin film (Park, Khachaturyan, and Priya 2012). Figure 3(b) shows room temperature dielectric constant electric field measurements performed for the PZT thin film annealed at 650 °C. The PZT film shows well defined butterfly-shaped behavior for the dielectric constant-voltage loop, which is characteristic of good ferroelectric behavior. A sharp increase in dielectric constant is observed with increasing electric field followed by an abrupt decrease in dielectric constant around the coercive field (Figure 3(b)). The observed behavior indicates the fast switching of domains with applied field. The inset of Figure 3(b) shows the AFM image of the PZT thin film deposited on Ni substrate at an annealing temperature of 650 °C. The surface morphology of the film is found to be fine having uniformly distributed grains of size close to 80 nm (inset of Figure 3(b)).The variation in phase and amplitude of the piezoresponse of PZT thin film as a function of applied sweep dc voltage from −10 V to 10 V is shown in Figure 4. A well-defined hysteresis loop was observed for both the phase and amplitude. The PZT thin film deposited on Ni substrate and annealed at 650 °C exhibits a significant piezoelectric response. It is inferred that the domain polarity could be successfully switched, and the observed phase change with the applied dc voltage swept from −10 V to +10 V is about 180 ° (Figure 4).

Figure 5 shows the dynamic characteristics of the magnetoelectric voltage coefficient based on PZT/Ni sample under longitudinal-transverse (L-T) mode. The magnetic field is applied longitudinally to the surface of PZT thin film as shown in the inset of Figure 5. The nickel substrate is strained due to magnetostrictive effect thereby inducing a stress in the piezoelectric PZT thin film. The strain is efficiently transferred from Ni to PZT thin film through elastic coupling via its coherent interface. The thin film laminate system (PZT/Ni) exhibited a good linear dc magnetic field bias response in the range of 0 Oe to 50 Oe which indicates the possible integration of PZT/Ni composite system for low level detection of dc

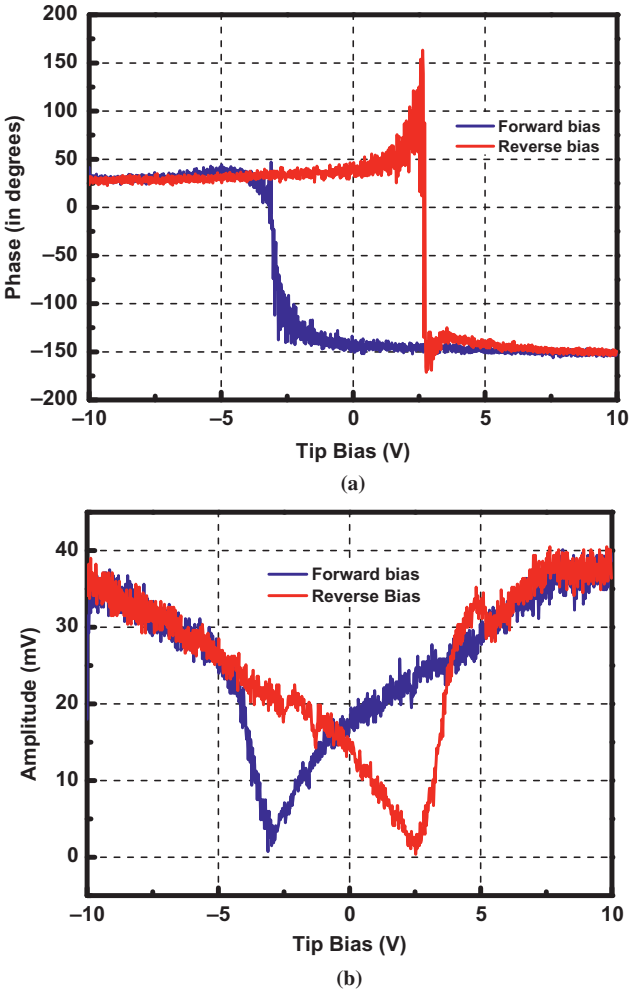

Figure 4: (a) and (b). The variation in phase and amplitude of the piezo response of PZT thin film with applied dc bias.

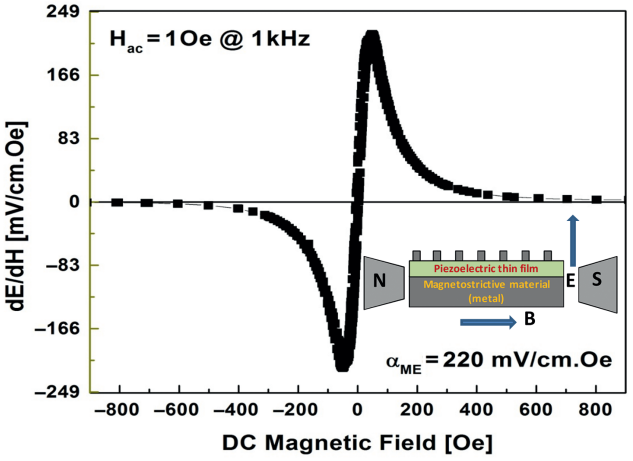

Figure 5: Magnetoelectric response of PZT thin film on nickel foil at Hac = 1 Oe. Inset shows the schematic of measurement technique in L-T mode.

magnetic field. At higher dc magnetic field strengths, the saturation in magnetostriction of nickel substrate gives rise to decrease in strain and hence a decline in magnetoelectric (ME) response is observed (Figure 5). The ME coefficient (α_{ME}) can be calculated as:

$$\alpha_{ME} = \frac{dV}{dH} \cdot \frac{1}{tH_{ac}}$$

where $\frac{dV}{dH}$ is the change in output voltage with respect to applied dc bias magnetic field, "t" is the thickness of the PZT thin film and "H_{ac}" is the superimposed AC magnetic field produced from Helmholtz coil. The estimated value of ME coupling coefficient is found to be about 220 mV/cm.Oe. The obtained value of ME coefficient is higher as compared to the corresponding value (140 mV/cm.Oe) reported by Park, Khachaturyan, and Priya (2012) using thin film of PZT over platinum coated-nickel zinc ferrite substrate. The low value of α_{ME} may be due to the clamping of the thin film by the substrate. The ME response obtained for the PZT thin film in the present study is also higher as compared to the recent reports available in the literature (Okazaki et al. 2013; Ryu et al. 2012; Lv et al. 2013). Better ME coupling is related to the good ferroelectric properties of the deposited PZT thin films and efficient strain transfer from underneath magnetostrictive nickel substrate. This is due to absence of any interfacial layer at the PZT-Ni interface which reduces the damping. The vibration damping is minimized at the PZT-Ni interface as the mechanical impedance for PZT (25–30 MRayl) and nickel (27 MRayl) are well matched (Bi, Zhang, and Fan 2007). Films high ME coefficient will find application in the field of energy harvesting,and can be exploited as magnetic field sensors and memory devices.

Conclusions

PZT thin films have been fabricated using chemical solution deposition technique and rapid thermal annealing process on magnetostrictive nickel substrate. Large magnetoelectric coefficient of 220 mV/cm.Oe has been obtained along with excellent ferroelectric characteristics.

Funding: One of the authors, RG, acknowledges Department of Science and Technology (DST), Government of India for the research fellowship and continuous support. The authors (Y. Z., A. C. and S. P.) gratefully acknowledge the financial support from the Office of Basic Energy Science, Department of Energy (DE-FG02-06ER46290). The exchange visit of R. G. at Virginia Tech was supported through NSF INAMM program.

References

Abdelghafar, K. K., K. Torii, T. Mine, T. Kachi, and Y. Fujisaki. 2000. "Orientation Control in PZT/Pt/TiN Multilayers with Various Si and SiO_2 Underlayers for High Performance Ferroelectric Memories." *Journal of Vacuum Science & Technology B* 18:231.

Ambika, D., V. Kumar, K. Tomioka, and I. Kanno. 2012. "Deposition of PZT Thin Films with {001}, {110}, and {111} Crystallographic Orientations and Their Transverse Piezoelectric Characteristics." *Advanced Material Letter* 3:102–6.

Bi, K., Z. L. He, and Y. G. Wang. 2012. "Hydrothermal Temperature Effect on Magnetoelectric Coupling of Ni/Pb($Zr_{0.52}Ti_{0.48}$)O_3 Bilayers." *Thin Solid Films* 520:5575–8.

Bi, Z., Z. Zhang, and P. Fan. 2007. "Characterization of PZT Ferroelectric Thin Films by RF-Magnetron Sputtering." *Journal of Physics: Conference Series* 61:120–4.

Bouregba, R., G. Poullain, B. Vilquin, and H. Murray. 2000. "Orientation Control of Textured PZT Thin Films Sputtered on Silicon Substrate with TiO_x Seeding." *Materials Research Bulletin* 35:1381–90.

Chashin, D. V., Y. K. Fetisov, K. E. Kamentsev, and G. Srinivasan. 2008. "Resonance Magnetoelectric Interactions Due to Bending Modes in a Nickel-Lead Zirconate Titanate Bilayer." *Solid State Communications* 148:55–8.

Chen, W., S. Shannigrahi, X. F. Chen, Z. H. Wang, W. Zhu, and O. K. Tan. 2010. "Multiferroic Behavior and Magnetoelectric Effect in $CoFe_2O_4$/Pb($Zr_{0.53}Ti_{0.47}$)O_3 Thick Films." *Solid State Communications* 150:271–4.

Dutschke, A., and J. Meinhardt. 2004. "Characterization of the Interface of PZT Sol–Gel Layers on Metallic Substrates." *Surface Interface Analysis* 36:1185–9.

Eerenstein, W., N. D. Mathur, and J. F. Scott. 2006. "Multiferroic and Magnetoelectric Materials." *Nature* 442:759–65.

Es-Souni, M., and A. Piorra. 2001. "On the Crystallization Kinetics of Solution Deposited PZT Thin Films." *Material Research Bulletin* 36:2563–75.

Foster, C. M., G. R. Bai, R. Csencsits, J. Vetrone, R. Jammy, L. A. Wills, E. Carr, and J. Amano. 1997. "Single-Crystal Pb(Zr_xTi_{1-x})O_3 Thin Films Prepared by Metal-Organic Chemical Vapor Deposition: Systematic Compositional Variation of Electronic and Optical Properties." *Journal of Applied Physics* 81:2349

Gilbert, J. M., and F. Galouchi. 2008. "Comparison of Energy Harvesting Systems for Wireless Sensor Networks." *International Journal of Automation and Computing* 5N4:334–47.

Gubinyi, Z., C. Batur, A. Sayir, and F. Dynys. 2008. "Electrical Properties of PZT Piezoelectric Ceramic at High Temperatures." *Journal of Electroceramic* 20:95–105.

He, Z. L., Y. G. Wang, and K. Bi. 2010. "Strong Magnetoelctric Coupling in a Ni-Pb($Zr_{0.52}Ti_{0.48}$)O_3 Bilyaer Derived from the Hydrothermal Method." *Solid State Communications* 150:1837–9.

Jeon, Y., R. Sood, L. Steyn, and S. G. Kim. 2003. "Energy Harvesting MEMS Devices Based on d33 Mode Piezoelectrioc Pb(Zr,Ti)O_3 Thin Film Cantilever." CIRP Seminar on Micro and Nano Technology, Copenhagen, Denmark, November 13–14.

Kambale, R. C., D. Patil, J. Ryu, Y. S. Chai, K. H. Kim, W. H. Yoon, D. Y. Jeong, D. S. Park, J. W. Kim, J. J. Choi, and C. W. Ahn. 2013. "Colossal Magnetoelectric Response of PZT Thick Films on Ni Substrates with a Conductive $LaNiO_3$ Electrode." *Journal of Physics D: Applied Physics* 46:092002.

Li, Z., J. Hu, L. Shu, Y. Gao, Y. Shen, Y. Lin, and C. W. Nan. 2012. "Thickness-Dependent Converse Magnetoelectric Coupling in Bi-Layered Ni/PZT Thin Films." *Journal of Applied Physics* 111:033918.

Lv, X., C. Cheng, Y. Xiao, M. Tang, Z. Tang, H. Cai, Y. Zhou, and R. Li. 2013. "Magnetoelectric $Pb(Zr_{0.52}Ti_{0.48})O_3$–$La_{0.65}Sr_{0.35}MnO_3$ Composite Thin Films Derived by the Pulse Laser Deposition Method." *Materials Letters* 100:7–10.

Marshall, J. M., Q. Zhang, and R. W. Whatmore. 2008. "Corona Poling of Highly (001)/(100)-Oriented Lead Zirconate Titanate Thin Films." *Thin Solid Films* 516:4679–84.

Martins, P., and S. L. Mendez. 2013. "Polymer-Based Magnetoelectric Materials." *Advanced Functional Materials* 23:3371–85.

Massad, J. E., and R. C. Smith. 2003. "A Domain Wall Theory for Hysteresis in Ferrroelectric Materials." *Journal of Intelligent Material Systems and Structures* 14:455–71.

McCorkle, P. 1923. "Magnetostriction and Magnetoelectric Effects in Iron, Nickel and Cobalt." *Physical Reviews* 22:271–8.

Meng, X. J., J. G. Cheng, B. Li, J. Tang, H. J. Ye, and J. H. Chu. 2000. "PZT Thin Films Derived from a Modified Sol-Gel Technique Based on Acetic Acid/Water System Using a New Zirconium Source." *Journal of Material Science Letters* 19:1967–9.

Misirlioglu, I. B., M. B. Okatan, and S. P. Alpay. 2010. "Asymmetric Hysteresis Loops and Smearing of the Dielectric Anomaly at the Transition Temperature Due to Space Charges in Ferroelectric Thin Films." *Journal of Applied Physics* 108:034105.

Oikawa, M., and K. Toda. 1976. "Preparation of $Pb(Zr,Ti)O_3$ Thin Films by an Electron Beam Evaporation Technique." *Applied Physics Letters* 29:491.

Okazaki, T., K. Mikami, Y. Furuya, Y. Kishi, Z. Yajima, and T. Kubota. 2013. "Magnetic Properties of Thin-Film Fe–Pd Alloy and Magnetoelectric Coupling in Fe–Pd/Ag/PZT/Ag/Fe–Pd Laminate Composites." *Journal of Alloys and Compounds* 577S:S300–4.

Pandey, S. K., A. R. James, R. Raman, S. N. Chatterjee, A. Goyal, C. Prakash, and T. C. Goel. 2005. "Structural, Ferroelectric and Optical Properties of PZT Thin Films." *Physica B* 369:135–42.

Park, C. S., A. Khachaturyan, and S. Priya. 2012. "Giant Magnetoelectric Coupling in Laminate Thin Film Structure Grown on Magnetostrictive Substrate." *Applied Physics Letters* 100:192904.

Park, C. S., S. W. Kim, G. T. Park, J. J. Choi, and H. E. Kim. 2005. "Orientation Control of Lead Zirconate Titanate Film by Combination of Sol-Gel and Sputtering Deposition." *Journal of material Research* 20:243.

Park, G. T., J. J. Choi, C. S. Park, J. W. Lee, and H. E. Kim. 2004. "Piezoelectric and Ferroelectric Properties of 1-μm-Thick Lead Zirconate Titanate Film Fabricated by a Double-Spin-Coating Process." *Applied Physics Letters* 85:12.

Patil, D. R., Y.Zhou, J. E. Kang, N. Sharpes, D. Y. Jeong, Y. D. Kim, K. H. Kim, S. Priya, and J. Ryu. 2014. "Anisotropic Self-Biased Dual-Phase Low Frequency Magneto-Mechano-Electric Energy Harvesters with Giant Power Densities." *APL Materials* 2:046102.

Patterson, A. L. 1939. "The Scherrer Formula for X-Ray Particle Size Determination." *Physical Review* 56:978–82.

Polcawich, R. G., and S. T. McKinstry. 2000. "Piezoelectric and Dielectric Reliability of Lead Zirconate Titanate Thin Films." *Journal of Material Research* 15:11.

Priya, S., and D. J. Inman, eds. 2009. *Energy Harvesting Technology*, 1st ed. New York: Springer.

Qiu, W., and H. H. Hng. 2002. "Effects of Dopants on the Microstructure and Properties of PZT Ceramics." *Materials Chemistry and Physics* 75:151–6.

Ryu, J., C. W. Baek, G. Han, C. S. Park, J. W. Kim, B. D. Hahn, W. H. Yoon, D. S. Park, S. Priya, and D. Y. Jeong. 2012. "Magnetoelectric Composite Thick Films of PZT–PMnN + $NiZnFe_2O_4$ by Aerosol-Deposition." *Ceramics International* 38S: S431–4.

Ryu, J., S. Priya, K. Uchino, and H. Kim. 2002. "Magnetoelectric Effect in Composites of Magnetostrictive and Piezoelectric Materials." *Journal of Electroceramics* 8:107–19.

Seifert, S., D. Sporn, T. Hauke, G. Muller, and H. Beige. 2004. "Dielectric and Electromechanical Properties of Sol-Gel Prepared PZT Thin Films on Metallic Substrates." *Journal of the European Ceramic Society* 24:2553–66.

Starner, T., and J. A. Paradiso. 2004. *Low Power Electronics Design*, Boca Raton, FL: CRC Press.

Vrejoiu, I., Y. Zhu, G. L. Rhun, M. A. Schubert, D. Hesse, and M. Alexe. 2007. "Structure and Properties of Epitaxial Ferroelectric $PbZr_{0.4}Ti_{0.6}O_3/PbZr_{0.6}Ti_{0.4}O_3$ Superlattices Grown on $SrTiO_3$ (001) by Pulsed Laser Deposition." *Applied Physics Letters* 90:072909.

Zhou, Y., D. J. Apo, and S. Priya. 2013. "Dual-Phase Self-Biased Magnetoelectric Energy Harvester." *Applied Physics Letters* 103:192909.

Zou, Q., H. E. Ruda, and B. G. Yacobi. 2001. "Improved Dielectric Properties of Lead Zirconate Titanate Thin Films Deposited on Metal Foils with $LaNiO_3$ Buffer Layers." *Applied Physics Letters* 78:1282.